Astron. Astrophys. 175, 151–163 (1987)

ASTRONOMY
AND
ASTROPHYSICS

The ultraviolet spectrum of the peculiar emission-line star GG Carinae*

E. Brandi[1], E. Gosset[2], and J.-P. Swings[2]

[1] Observatorio Astronomico, Universidad Nacional, Paseo del Bosque, 1900 La Plata, Argentina
[2] Institut d'Astrophysique, Université de Liège, 5, avenue de Cointe, B-4200, Cointe-Ougrée, Belgium

Received June 11, accepted September 12, 1986

Summary. This paper presents the first study of the properties of the peculiar emission-line star GG Carinae in the ultraviolet wavelength domain.

From IUE high resolution spectra, we investigate the behaviour of different ions concerning their respective profiles as well as their radial velocities. A large number of ionization stages are actually simultaneously present. The ultraviolet spectrum is dominated by absorptions, mainly of Fe II; but emissions are also present in some lines of O I, Mg II, Fe II. The absorption line widths increase with the ionization stages. No correlation appears between the radial velocities and the excitation potential whereas some correlation exists between the former and the ionization potentials. A Bowen mechanism is responsible for the observed emission (P Cyg type profile) of the resonance triplet of O I as well as for the resonance doublet of Mg II. In the far UV, Fe II is characterized by the presence of absorption lines with the remarkable exception of multiplet 191 which shows P Cyg profiles: these are explained as being due to a radiative pumping mechanism. In the near UV, Fe II is characterized by double absorption lines with sometimes a complex emission feature on the redward side. It is also shown that resonance fluorescence is the main excitation of the Fe II emission in the near ultraviolet, in the optical and in the infrared regions.

From IUE low resolution data, we propose a value of the $B-V$ excess of $E_{B-V} = 0.52 \pm 0.04$ (2σ). The continuum of GG Car from the UV to the visible is rather well represented by the theoretical flux of a $T_{\rm eff} = 18{,}000$ K Kurucz standard model atmosphere. We investigate also the ultraviolet light curve, which is essentially similar to the one observed in the visible (Gosset et al., 1984, 1985).

Identifications of the lines in the UV spectrum of GG Car covered by IUE are being published separately (Brandi and Gosset, 1986) in the Supplement Series of this Journal.

Key words: stars: GG Car – UV radiation – stars: emission-line – stars: variable – stars: eclipsing binaries

Send offprint requests to: E. Gosset

* Based on observations with the International Ultraviolet Explorer

1. Introduction

GG Car ($\alpha = 10^{h}53^{m}58^{s}$; $\delta = -60°07'.5$ (1950.0); HD 94878 = CD $-59°3425$ = CPD $-59°2855$ = MWC 215 = Wra 691 = He 3-526) has been known early as an object displaying a peculiar spectrum with bright emission lines (Pickering 1896a,b; Cannon, 1915). It is included in the Henry Draper Catalogue as belonging to the P Cyg type and in other lists of emission-line stars, e.g. the list of P Cyg stars by Beals (1951) and the low-dispersion catalog of emission-line objects by Sanduleak and Stephenson (1973, where GG Car is object n°26).

After the first description by Smith (1955) of a low dispersion spectrogram of GG Car as a purely emission spectrum of H and Fe II, further spectroscopic studies in the visual region indicated that the spectrum of GG Car showed emission lines of H, Fe II and [Fe II] (Carlson, 1968; Swings, 1974; Carlson and Henize, 1979; Hernandez et al., 1981; Gosset et al., 1985). A resolution into two components for the Fe II lines as well as a P Cyg profile at H_γ was detected by Swings (1974), while Hernandez et al. (1981) and Gosset et al. (1985) indicated P Cyg profiles of Beals type III for all the Balmer lines up to H_{21}.

The light variability of GG Car was first investigated by Kruytbosch (1930) with, as a result, a period of 31.043 days, and it was emphasized that one might possibly be dealing with a star "which is at the same time an eclipsing system and a genuine variable". Other investigations of the light variability of GG Car were performed by Hoffleit (1933), Greenstein (1938), Gaposchkin (1953), Chen et al. (1983) and Gosset et al. (1984). The last one consists of extensive photoelectric photometry in both the standard UBV and Strömgren uvby systems. A Fourier analysis of these data leads to the determination of a period of $31^{d}.020$. However, because of different physical arguments, the authors suggested that the true period could be $62^{d}.039$ i.e. about twice as long as that reported by Kruytbosch (1930). Similar periods had been mentioned by Hoffleit (1933) and Greenstein (1938). On the basis of radial velocity measurements of the H absorptions, Hernandez et al. (1981) gave a higher priority to a 31-day period rather than to a 62-day one.

Gosset et al. (1984, 1985) have attempted to derive a physical model of GG Car on the basis of both their photometric data and their spectroscopic results; the latter, i.e. the radial velocities along the lightcurve definitely showed that the period was 31.02 days. GG Car remains, however, a puzzling stellar "system" for which Gosset et al. (1984, 1985) summarized the main charac-

teristics that are to be taken into account: a) The spectrum of GG Car exhibits permitted and forbidden emission lines and P Cyg profiles for most of the Balmer lines during the whole lightcurve. These lines must originate in an envelope around the primary star and be accelerated outwards; b) Since the radial velocities show different variations from line to line, as well as between emission and absorption components of the same transition, the stratified envelope is not spherically symmetric but, rather, is elongated; c) Absorption lines of He I as well as a second absorption component of the Balmer lines appear around phase 0.45 ($P = 31^{d}.020$), at the time that a possible partial occultation ("glitch") in the lightcurve is observed; d) Smaller scale variabilities are also probably present in the main trend of the light variation observed in GG Car, thus tending to confirm that at least one of the components could be a genuine variable (Kruytbosch, 1930); e) The radial velocities analysed in terms of a binary system give a mean eccentricity of 0.3 and a mass function of order 0.02, indicating that the star we see is the most massive of the system: these values are of course to be taken with caution, as indicated in Gosset et al. (1985).

Finally, it is known that GG Car has an infrared excess of the type that appears to be associated with circumstellar dust (Allen, 1973; Cohen and Barlow, 1980; Bouchet and Swings, 1982).

The aim of this paper is to present the first study of low and high resolution IUE ultraviolet spectra of GG Car. The continuum and the line spectra are analysed and discussed in details in the next sections. The behaviour of the different ions and their radial velocities are described while a separate publication, in the Supplement Series (Brandi and Gosset, 1986), gives the line identifications between 1230 and 3200 Å.

2. Observations

High and low dispersion spectral images, for both the long- and the short-wavelength regions were obtained with the International Ultraviolet Explorer Satellite (IUE: see Boggess et al. (1978a,b), Holm (1982)). The images have been acquired between 1978 and 1982 at the Villafranca del Castillo Satellite Tracking Station of the European Space Agency (Vilspa). The log of all the observations is given in Tables 1a and 1b for the high and the low resolution data respectively. The extraction and processing of all the spectra has been performed using the up-to-date (Vilspa, December 1985) version of the Standard Image Processing Software. Absolute flux calibrations of the low resolution spectra were based on the paper of Bohlin and Holm (1981) whereas for the approximate absolute calibrations of high resolution spectra, the paper by Cassatella et al. (1981) was taken as the reference.

3. Description of the high resolution spectrum

3.1. The line spectrum

The ultraviolet spectrum of GG Car consists essentially of a very large number of absorption features and of a few P Cyg profiles for the resonance lines of Mg II, O I (multiplet 2) and for several Fe II multiplets.

Table 1a. High resolution UV spectra of GG Carinae

IUE Image	Date			Aperture	Exposure time (Seconds)	Observer	Phase (Gosset et al., 1985)
	yr	m	d				
LWR 4920	1979	06	30	*L*	9000	Klutz	0.38
LWR 5741	1979	10	03	*L*	9000	Swings	0.46
SWP 8936	1980	05	06	*L*	25,200	Klutz	0.41

Table 1b. Low resolution UV spectra of GG Carinae

IUE Image	Date			Aperture	Exposure time (Seconds)	Observer	Phase (Gosset et al., 1985)
	yr	m	d				
LWR 2396	1978	09	18	*L*, *S*	600, 3600[a]	Swings	0.22
LWR 2397	1978	09	18	*L*	120	Swings	0.22
SWP 2685	1978	09	18	*L*	1800	Swings	0.22
SWP 2686	1978	09	18	*L*	240	Swings	0.22
LWR 4921	1979	06	30	*L*, *S*	180, 210	Klutz	0.38
SWP 5679	1979	06	30	*L*, *S*	600, 780	Klutz	0.38
SWP 6737	1979	10	03	*L*, *S*	480, 780	Swings	0.46
LWR 7683	1980	05	06	*L*, *S*	180, 210	Klutz	0.41
LWR 8071	1980	06	18	*L*, *S*	120, 720[b]	de Boer	0.82
SWP 9309	1980	06	18	*L*, *S*	300, 420[b]	de Boer	0.82
LWR 14625	1982	11	14	*L*	180	Skillen	0.15
SWP 18555	1982	11	14	*L*	600	Skillen	0.15

[a] Saturated
[b] True exposure times

The ultraviolet line spectrum of GG Car shows a great variety of ionization stages, ranging from O I, S I, Mg I to the superionized elements such as C IV and Si IV. The singly ionized elements undoubtedly dominate the spectrum, mainly Fe II, and in order of decreasing number of identified lines, Ni II, Si II, Al II, S II, Mg II, Zn II, C II, and perhaps Cu II. Doubly ionized elements are definitely present such as Fe III, Al III, Ti III, Ni III and P III.

The pure absorption lines, including C IV and Si IV, are in general symmetric, and their widths are different for the different groups of elements, and increase as one moves towards the more highly ionized ones.

Some lines are multiple: the discussion concerning the origin of the different components is deferred to Sect. 3.4. The behaviour of the elements and ions shows the following characteristics:

C I: Sharp and undisplaced lines arising from the lower levels are present in the short wavelength spectrum (Fig. 1). A similar behaviour is seen for S I and Cl I. These lines probably are of interstellar origin.

C II: The lines of C II at $\lambda\lambda$ 1334.53, 1335.71 and 1335.66 Å are strong – near saturation – and broad; for that reason it is impossible to separate both components. Contributions of sharp interstellar lines seem to be present, as well as that of P III λ 1334.87.

O I: The three lines of multiplet 2 are present and one of these is blended with Si II λ 1304.37; O I shows P Cyg profiles except at λ 1302.17 which comes from level 0.00 eV and is characterized by two absorptions of which the one towards the longer wavelengths (unfortunately affected by a reseaux mark) may absorb the emission component (Fig. 2).

Mg I: The only line present is λ 2852.13 with two well separated absorption components, of which one is almost undisplaced and probably of circumstellar origin.

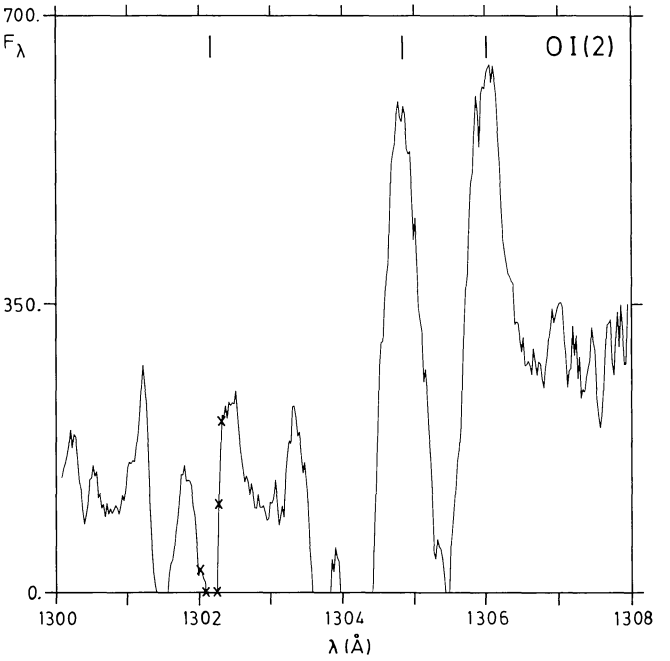

Fig. 2. Multiplet 2 of O I in the UV spectrum of GG Car, exhibiting P Cyg profiles. The crosses indicate points affected by reseaux marks

Mg II: These resonance lines also display P Cyg profiles with a strong emission and two absorption components (Figs. 3, 4). The broad violet component (FWHM $\simeq$ 1.2 Å) looks slightly asymmetrical but contributions due to Fe II are present. The sharp red absorption (FWHM $\simeq$ 0.6 Å) is similar to those almost undisplaced absorption components that are present in the

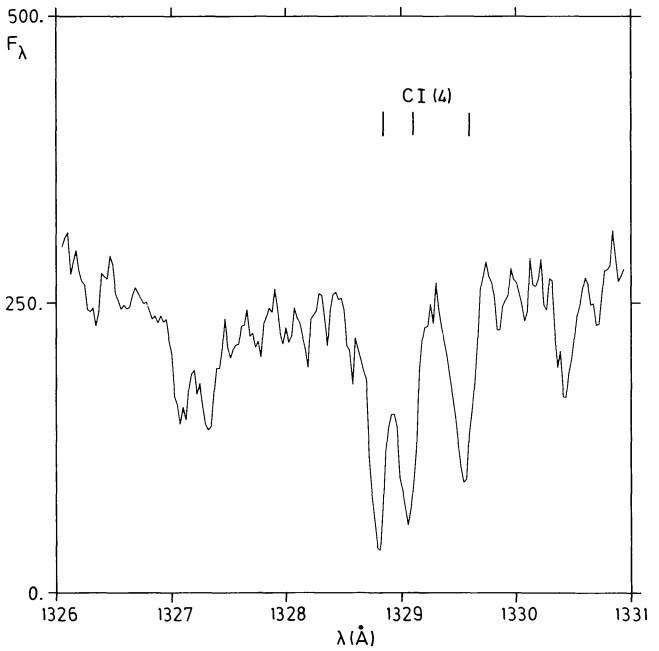

Fig. 1. Sharp undisplaced lines (probably of interstellar origin) of C I (multiplet 4) in the UV spectrum of GG Car. The vertical bars indicate the positions of rest wavelengths. The ordinates give the flux in units of 10^{-14} erg cm^{-2} s^{-1} Å^{-1} (this unit is that of the other relevant figures as well)

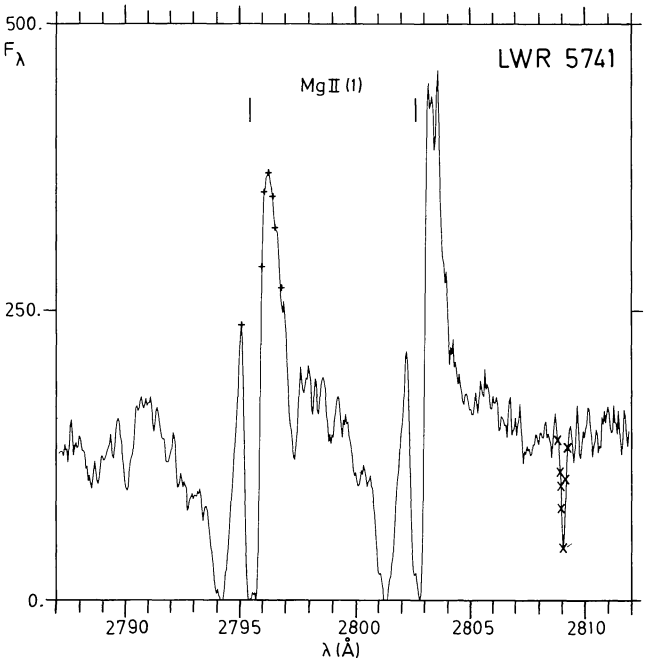

Fig. 3. The resonance multiplet of Mg II in the UV spectrum of GG Car (phase φ = 0.46). Plus signs indicate pixels at or very near saturation

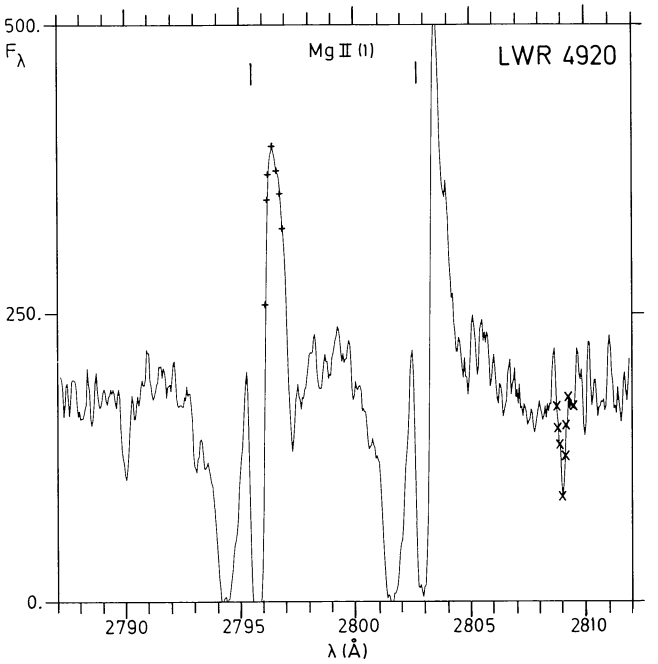

Fig. 4. As for Fig. 3, with phase $\varphi = 0.38$

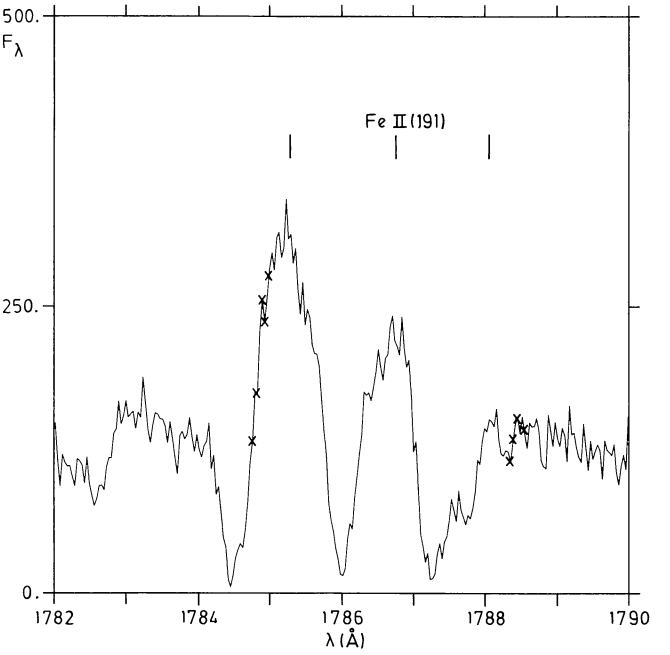

Fig. 5. Multiplet 191 of Fe II in the UV spectrum of GG Car. See text for details

lines arising from the 0.00 eV level of O I, Mg I, Fe II, Al II, Al III, Ni II, Si II, Ti III and Zn II. The presence of this component is also reported in the binary system AX Monocerotis (Sahade and Brandi, 1985) and in the B[e] star HD 87643, De Freitas Pacheco et al. (1985) observe similar "zero-volt" absorptions of Mg I, Mg II, Mn II and Fe II. Subordinate Mg II lines of multiplets 2 and 3 (4.4 eV) are present as single absorptions with no outstanding emission.

Fe II: In the UV spectrum the Fe II lines display a complex behaviour, since several kinds of profiles such as pure and single absorptions, emissions, and P Cyg profiles with different characteristics are represented. In May 1980 (SWP 8936) the Fe II shows narrow and symmetrical lines in absorption (FWHM $\simeq$ 0.6 Å) except multiplet 191 which shows typical P Cyg profiles. The most prominent emission in the triplet is that of the λ 1785.26 component and a contribution of Ni II at λ 1788.49 seems to extinguish the emission in the third component (Fig. 5).

In June and October 1979 (LWR 4920 and LWR 5741 respectively) the Fe II lines, which are the main contributor in the near UV spectrum, show P Cyg profiles with different structures compared to those of multiplet 191. They are composed of two absorptions separated by approximately 40 km s^{-1} and with complex emission features on the long wavelength side (Fig. 6); the presence of the double structure could possibly be an effect of increased resolution at the longer wavelengths. The emission intensity changes for the different multiplets, as described in the next section; the Fe II lines arising from the 0.00 eV level have also the longward absorption component (Fig. 7).

Ni II: Alike the Fe II absorptions, Ni II seems to have only one component in the far UV and two components in the near UV. Unfortunately, the strongest lines of Ni II longward of 2000 Å are in a region of very low signal to noise ratio.

Al II, Si II, S II, Zn II and possibly Cu II are the other singly ionized elements identified in the spectrum of GG Car. These lines only display one stellar component in absorption.

P II: exhibits a few lines.

Cr II: It is faintly present through the resonance lines, but these are blended or poorly defined.

Mn II: It is present through three sharp undisplaced lines ($\lambda\lambda$ 2576.11, 2593.72, 2605.68 Å of multiplet 1). They seem to be of interstellar origin.

Fe III and Ni III have no resonance lines in the IUE wavelength range but several subordinate lines of these ions are present.

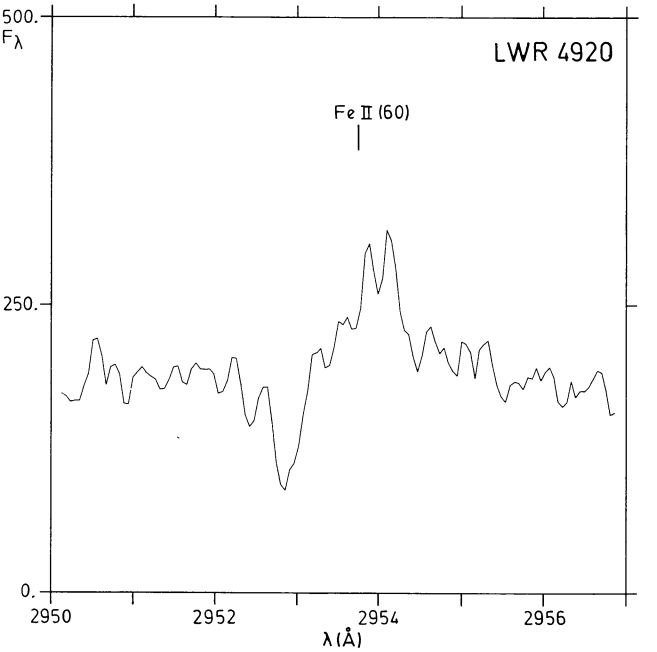

Fig. 6. The λ 2953.8 Å line of Fe II (multiplet 60) exhibiting several absorption and emission components

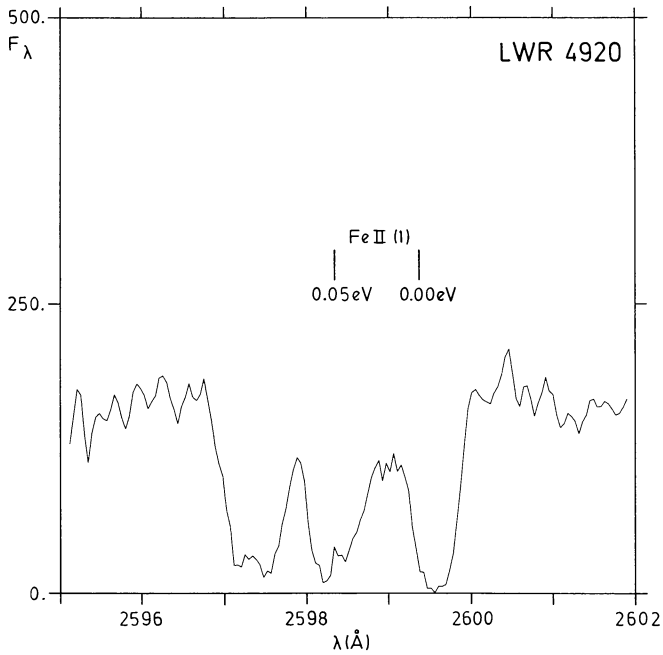

Fig. 7. Example of two Fe II lines from multiplet 1. The two lines exhibit double displaced absorption; the essentially undisplaced absorption component of the zero level line should be noted as well

Fe III: displays single profiles which are wider than those of the Fe II lines (FWHM $\simeq$ 1.2 Å). The ion is represented by the strongest transitions of multiplets whose lower levels have energies between 3.7 eV and 8.6 eV.

Ni III: has profiles like those of Fe III; lines from several multiplets are seen.

Al III, Ti III and P III display their resonance lines with a single, although fairly broad, absorption profile. They also display a sharp component in the transitions arising from the 0.00 eV level, although we cannot tell whether the same is true for the case of P III because that line coincides with the resonance line of C II.

Si III: is present through a few lines coming from excited levels.

Si IV: The two lines of multiplet 1 are present. They are broad (FWHM $\simeq$ 2.7 Å) and symmetrical (Fig. 8).

C IV: The two lines of multiplet 1 form a unique broad profile (FWHM $\simeq$ 6 Å) (Fig. 9).

It should be mentioned that at $\lambda\lambda$ 1242.5 and 1247.1 Å there are two broad lines whose profiles resemble those of Si IV. The feature seen near 1247.1 Å could be due to C III (9) at 1247.38 Å. The other one remains unidentified, but if we consider the two resonance lines of NV as possible, an unlikely redshift of about 1000 km s^{-1} would be implied in order to match the observations!

3.2. Radial velocities

Table 2 presents a summary of the velocity shifts of the resonance and subordinate lines of the different elements and ions present in the UV spectrum of GG Car. The data of this table are the mean heliocentric radial velocities in km s^{-1}, measured in SWP and LWR parts of the spectrum, for all unblended lines of the different ions, together with their standard deviation (σ) and the number of measured lines (n).

The precision of the radial velocity determinations is limited by the IUE resolution and by the difficulty to measure the line center. An error of about $\pm$15–20 km s^{-1} is to be expected considering the resolution of the spectrograph and, as can be judged from experience, an inaccurate estimation of the line center is at least of the same order. Systematic differences among the velocities in the three images probably due to uncertainties in the calibration procedure are seen: therefore, only the relative values must be considered as significant.

In Table 3 we list for each relevant multiplet the mean radial velocities for all Fe II and Ni II unblended lines, versus the mean energy involved in the transition.

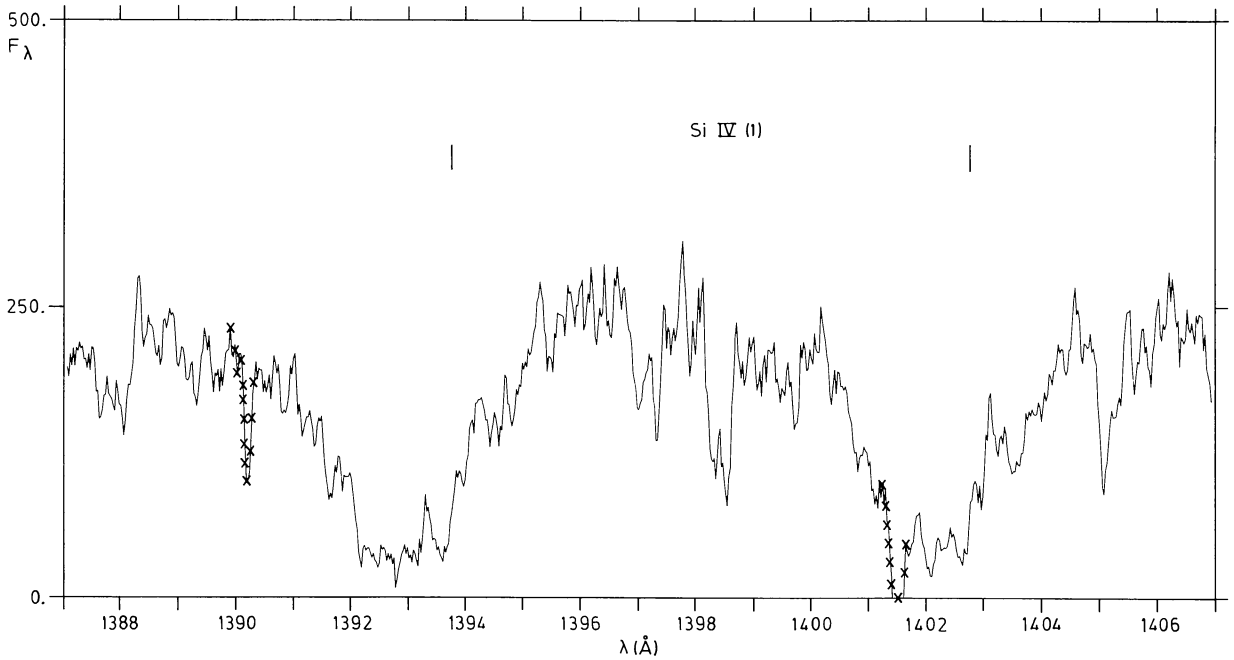

Fig. 8. The two resonance lines of Si IV appear as broad quasi-saturated absorptions in the UV spectrum of GG Car

Table 2. Mean radial velocities (km s^{-1}) of the absorption lines in the spectrum of GG Carinae

	SWP 8936						LWR 4920[2]						LWR 5741[2]					
	Resonance Lines[1]			Subordinate L.			Res. L.[1]			Sub. L.			Res. L.[1]			Sub. L.		
	$\bar{V}$	σ	n	$\bar{V}$	σ	n	$\bar{V}$	σ	n	$\bar{V}$	σ	n	$\bar{V}$	σ	n	$\bar{V}$	σ	n
C I	+10	5	9															
S I	+6	4	4															
Mg I							−87		1				−108		1			
							+39*x*		1				+8*x*		1			
O I	−138	17	3															
	+7*x*		1															
C II	−139*b*		1															
Mg II							−120	2	2	−73	7	4	−157	5	2	−65	10	4
							+31	1	2				+10	2	2			
Al II	−69*b*		1	−84	19	3												
	+2																	
Si II	−123	15	7															
	−2	0.7	2															
S II	−137	15	3															
Fe II	−109	17	17	−104	14	91	−132	9	27	−135	9	26	−161	15	22	−161	11	22
	+0.5		2				+23	2	4				+2	1	3			
							(−94)	8	25	(−87)	5	26	(−113)	31	23	(−119)	7	22
Ni II	−97	9	10							−112	12	12				−128	12	9
	+11	6	5							(−76)	9	12				(−75)	16	8
Zn II	−121	6	2															
	+8	8	2															
Al III	−146*b*	8	2															
	−21	3	2															
P III	−98		1															
Ti III	−82	14	4	−94	7	2												
Fe III				−125	23	18												
Ni III				−119	26	3												
Si IV	−168	16	2															
	−11:		2															

[1] The velocities of the components arising from the 0.00 eV level are indicated in a second line for each element

[2] In the case of Ni II and Fe II the velocities of the other component observed in the LWR region are indicated in parentheses

b Blended lines; *x* reseaux mark in the line; : doubtful

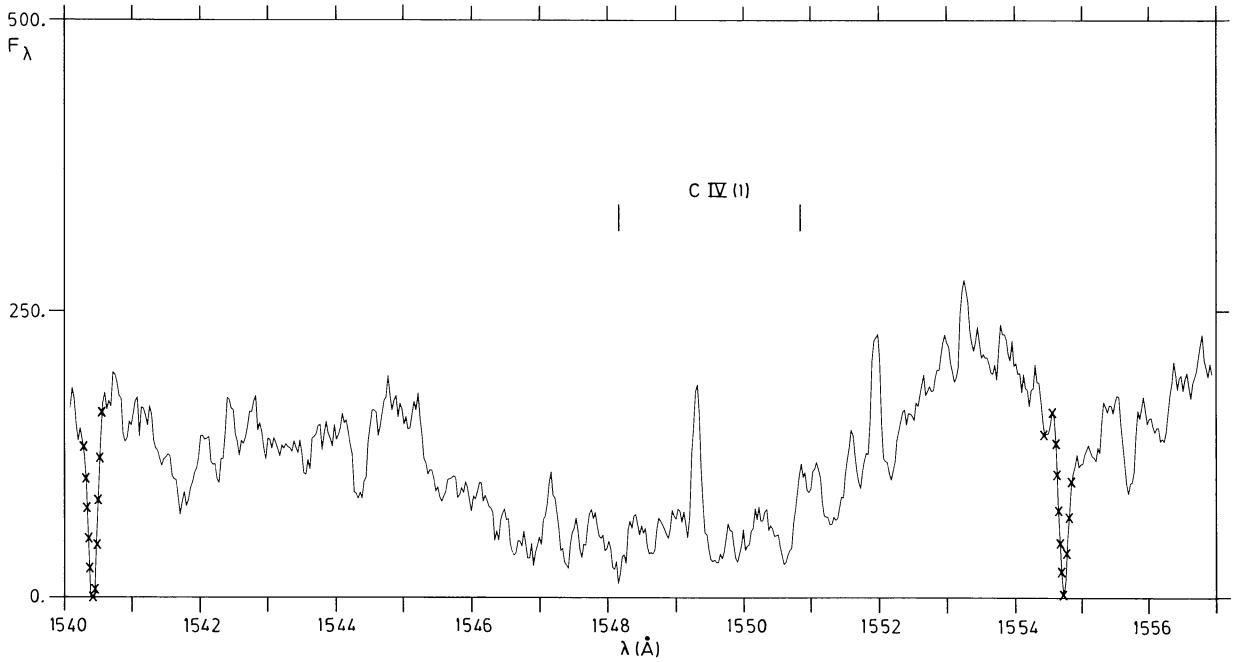

Fig. 9. The two resonance lines of C IV appear as broad and blended. The two narrow emissions peaking at $\lambda\lambda$ 1549.3 and 1551.9 Å are due to spikes and have no astrophysical meaning

Table 3. Radial velocities extracted from the ultraviolet lines. χ_{LL} = lower level mean energy. χ_{UL} = upper level mean energy

Fe II	SWP 8936			
Multiplet	No. of lines	$\bar{V} \pm \sigma$ (km s^{-1})	χ_{LL} (eV)	χ_{UL} (eV)
UV 8	9	−113 ± 16	0.08	7.7
UV 9	6	−110 17	0.08	9.8
UV 38	5	−95 13	0.34	7.5
UV 40	6	−110 9	0.34	7.8
UV 41	5	−99 5	0.34	7.7
UV 42	4	−115 12	0.32	7.8
UV 43	7	−116 15	0.31	7.9
UV 44	6	−104 18	0.31	8.1
UV 45	5	−106 28	0.32	8.2
UV 68	6	−111 12	1.05	8.6
UV 85	2	−101 3	1.66	8.9
UV 88	1	−94	1.66	11.2
UV 98	2	−94 0.7	1.99	8.7
UV 99	2	−99 6	1.99	8.9
UV 101	2	−111 17	1.99	9.0
UV 102	2	−94 11	1.99	9.3
UV 125	3	−106 15	2.55	9.1
UV 140	1	−101	2.53	9.0
UV 141	1	−109	2.53	9.2
UV 142	2	−98 6	2.58	9.4
UV 170	2	−88 7	2.68	9.0
UV 191	3	−113 7	2.88	9.8
UV 193	3	−98 13	2.88	11.3

As illustrated in Fig. 10(a), (b) and (c) for the three epochs, no correlation between the radial velocity and the excitation potentials can be found for the Fe II and Ni II absorption lines. Therefore, only a weak temperature variation may, at most, exist between the regions where these lines are formed. If we include the Mg II values (from Table 2) in the LWR graphics, there is a correlation in the sense that the resonance lines (mult. UV 1) are more blueshifted than the subordinate lines (mult. UV 2 and 3).

In the photographic region, the velocities of the Balmer lines are clearly a function of the excitation potential (Gosset et al., 1985).

Figure 11 shows the mean radial velocity of the elements in SWP image versus the sum of the ionization potentials from the neutral to the given state. The velocities are seen to decrease with the ionization. The values for P III and C II can suffer from large uncertainties. The velocities for P III have been computed from only one line of multiplet 1 and the velocity for C II is derived from the strongly blended triplet $\lambda\lambda$ 1334.53, 1335.71 and 1335.66 Å which also contains the contribution due to P III at λ 1334.87 Å. The velocity of Ti III does not fit the apparent dependence on the ionization potential. The correlation is more significant for the lines due to the singly ionized elements.

3.3. Interpretation of the emission lines

3.3.1. Fe II emission lines

Fe II is the dominant element in the UV spectrum of GG Car particularly in the long wavelength region. Its behaviour seems to be in general complex: in the far UV, Fe II is characterized by the presence of absorption lines, except for the multiplet 191 which shows P Cyg profiles; in the LWR region, the Fe II lines begin to develop emissions toward the long wavelengths. The emissions

Table 3 (continued)

Fe II	LWR 4920					LWR 5741		
Multiplet	No. of lines	$\bar{V}_B \pm \sigma$	$\bar{V}_R \pm \sigma$	χ_{LL}	χ_{UL}	No. of lines	$\bar{V}_B \pm \sigma$	$\bar{V}_R \pm \sigma$
UV 1	9	−130 ± 6	−96 ± 6	0.06	4.8	9	−164 ± 12	−129 ± 16
UV 2	4	−141 3	−91 10	0.09	5.2	4	−163 15	−116 30
UV 3	4	−128 11	−90 9	0.08	5.3	4	−138 11	−71 7
UV 35	2	−120 9	−89	0.34	5.6	2	−154 2	−116 2
UV 60	2	−136 6	−85 6	1.01	5.2	2	−163	−126 5
UV 62	2	−133 2	−95 5	1.04	5.6	2	−160 10	−122 18
UV 63	3	−128 9	−87 3	1.05	5.6	3	−149 22	−117 14
UV 64	6	−135 18	−95 18	1.05	5.9	6	−153 19	−106 26
UV 78	3	−140 21	−82 6	1.69	5.9	3	−169 24	−123 4
UV 234	2	−151 0.7	−86 0.7	3.24	7.7	2	−156 8	−119 0.7
UV 235	2	−130 0.7	−81 7	3.24	7.7	2	−152 0.7	−124 8
UV 261	1	−132	−87	3.37	7.9	1	?	−110
UV 263	2	−146 22	−85 2	3.39	8.0	1	−165	−120
UV 283	1	−129	−84	3.80	8.4	1	−185	−129
Ni II	SWP 8936							
UV 4	2	−105 0.7		0.10	7.2			
UV 5	3	−92 10		0.06	7.2			
UV 7	1	−87		0.19	8.4			
UV 8	3	−104 9		0.08	9.1			
UV 10	1	−107		0.00	9.4			
	LWR 4920							
UV 11	1	−112	−74	1.15	6.5			
UV 12	2	−98 8	−71 8	1.10	6.6			
UV 22	1	−128	−77	1.85	7.1			
UV 13	1	−111	−84	1.10	6.8			
UV 18	1	−116	−92	1.76	6.6			
UV 19	2	−107 22	−76 13	1.76	6.8			
UV 20	1	−126	−75	1.67	7.0			
UV 36	1	−107	−69	3.07	8.2			
UV 50	2	−117	−72	3.65	8.9			

in the multiplets 60, 62, 63 and 78 are stronger than those seen for the resonance lines. Nevertheless, multiplets 35 and 36 whose transitions have the common metastable lower level a^4F, are only observed in absorption. At the long wavelength side of the LWR images, some lines corresponding to the visual multiplets, specially the line at λ 3196.07 (V7), show a clear emission.

Besides, it is known that in the photographic region, GG Car presents many Fe II emission lines (Carlson, 1968; Swings, 1974; Carlson and Henize, 1979; Hernandez et al., 1981; Gosset et al., 1985). One (unpublished) observation of GG Car obtained with the ESO Reticon system attached to the spectrograph at the Cassegrain focus of the 3.6 m telescope, shows conspicuous Fe II emission lines (mult. V40, 46, 73, 74) in the range from 5800 Å to 11,000 Å. A similar phenomenon was observed in the B[e]p star HD 45677 (Swings, 1979; Selvelli and Stalio, 1980), in the symbiotic star CH Cyg (Hack and Selvelli, 1982) and in the B[e] star HD 87643 (De Freitas Pacheco et al., 1985), showing in each case large differences in the complex Fe II emission/absorption spectrum.

The explanation of this particular behaviour would require a complete knowledge of the excitation mechanism of the Fe II emission spectrum. Because this is not fully known, only a qualitative interpretation can be worked out for the case of GG Car as for the above-mentioned stars: a continuum fluorescence mechanism is suggested. According to such a mechanism, excitation of the far UV multiplets is followed by decay through near UV, visible and near IR multiplets. Transitions between a low lying level and an upper level of high energy ($\gtrsim$5.5 eV) are indeed observed only in absorption (e.g. mult. 8, 9, 38, 40, 41, 68, 35 and 36). On the other hand, transitions involving an upper level with an energy $\lesssim$5.5 eV do exhibit some emission due to photons in transit decaying from the overpopulated higher levels (e.g. mult. 60, 62, 63, 64, 78). Figures 12 and 13 give examples of Fe II lines relevant to each type of transition. An explanation of the

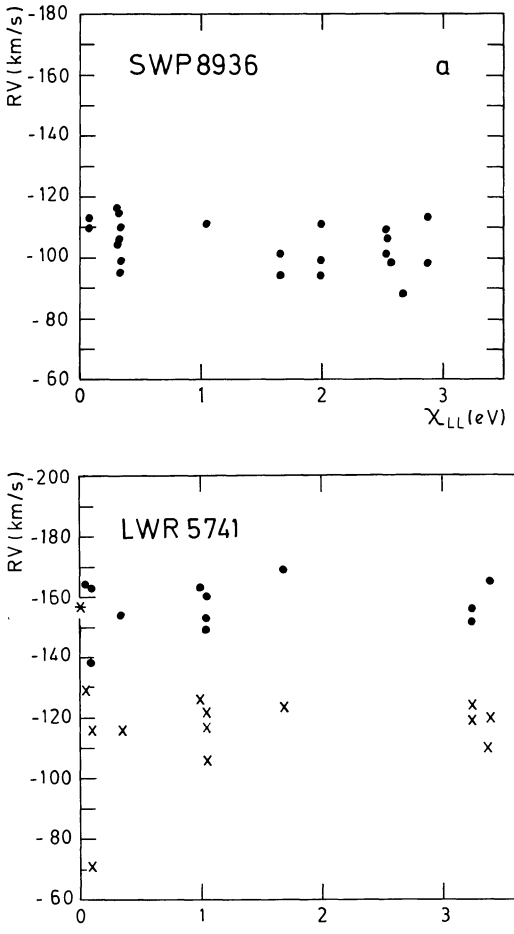

Fig. 10a–c. Relative radial velocities of absorption lines with respect to their excitation potential (LL = lower level), for the 3 different spectra, i.e. **a** corresponding to $\varphi = 0.41$ (short wavelength Fe II lines); **b** to $\varphi = 0.38$ (long wavelengths); and **c** to $\varphi = 0.46$ (long wavelengths). The following symbols are used: ★ for Mg II, ● for Fe II (B), × for Fe II (R), ○ for Ni II (B), and + for Ni II (R); B and R respectively refer to the blue or red component of the double absorption

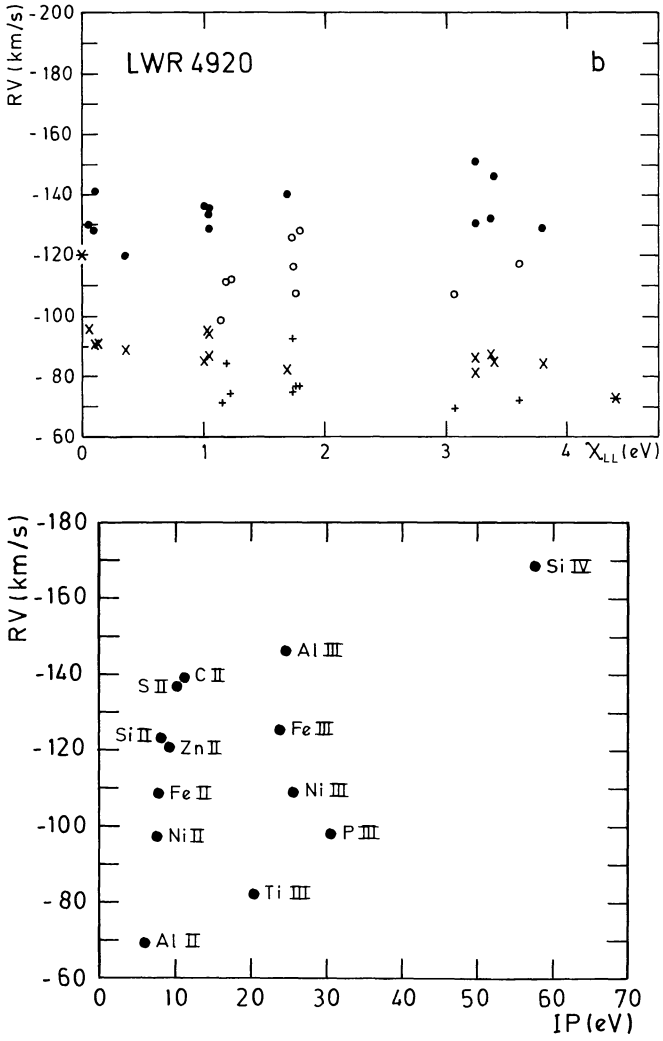

Fig. 11. Mean relative radial velocities of lines of different ions with respect to their ionization potential

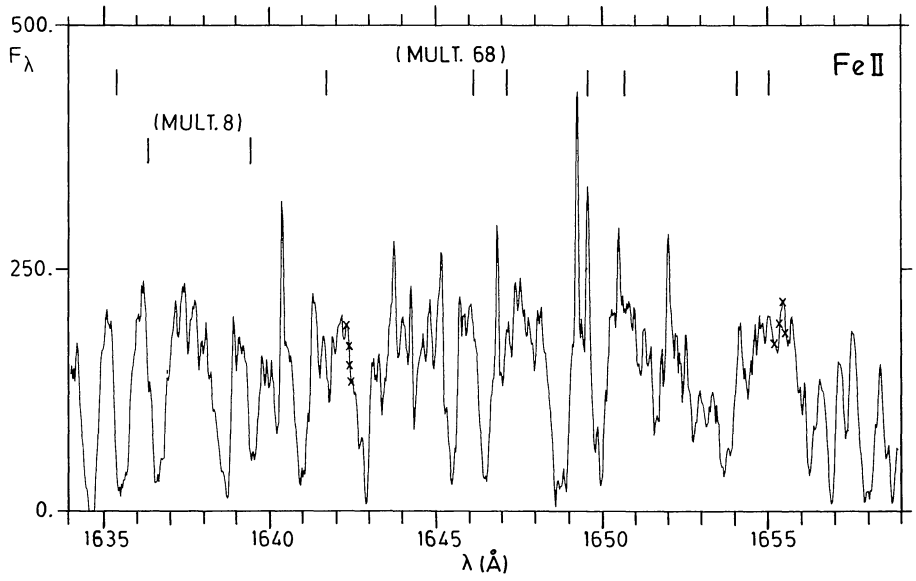

Fig. 12. Portion of the far UV spectrum of GG Car: representative Fe II lines of multiplets 8 ($a^6D - y^6P^0$) and 68 ($a^4D - y^4P^0$) appearing only in absorption. No contribution due to a decay from higher levels exists in these lines

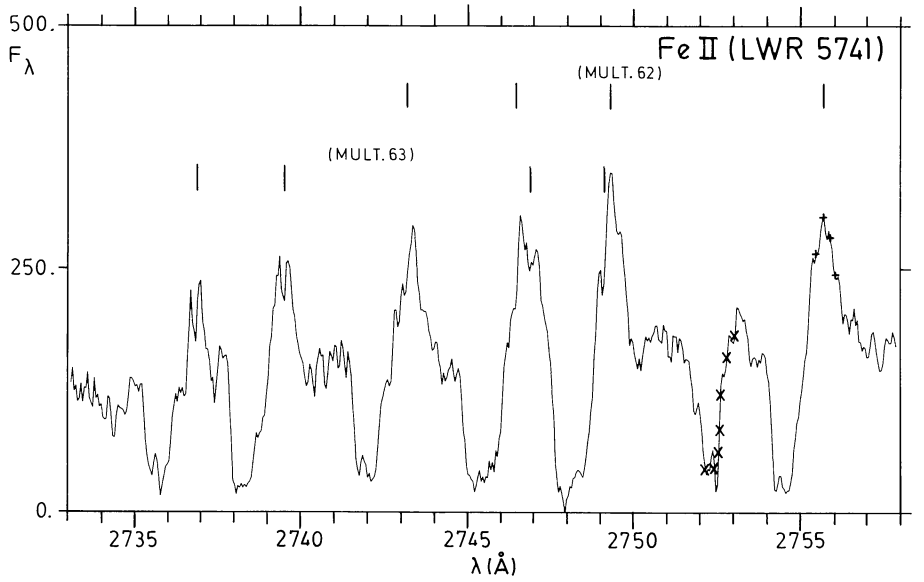

Fig. 13. Portion of the near UV spectrum of GG Car: Fe II lines of multiplets 62 and 63 exhibiting emission components as well as more or less well marked double absorptions. Here, contrary to the cases of Fig. 12, additional contributions from decays from higher levels are clearly observable

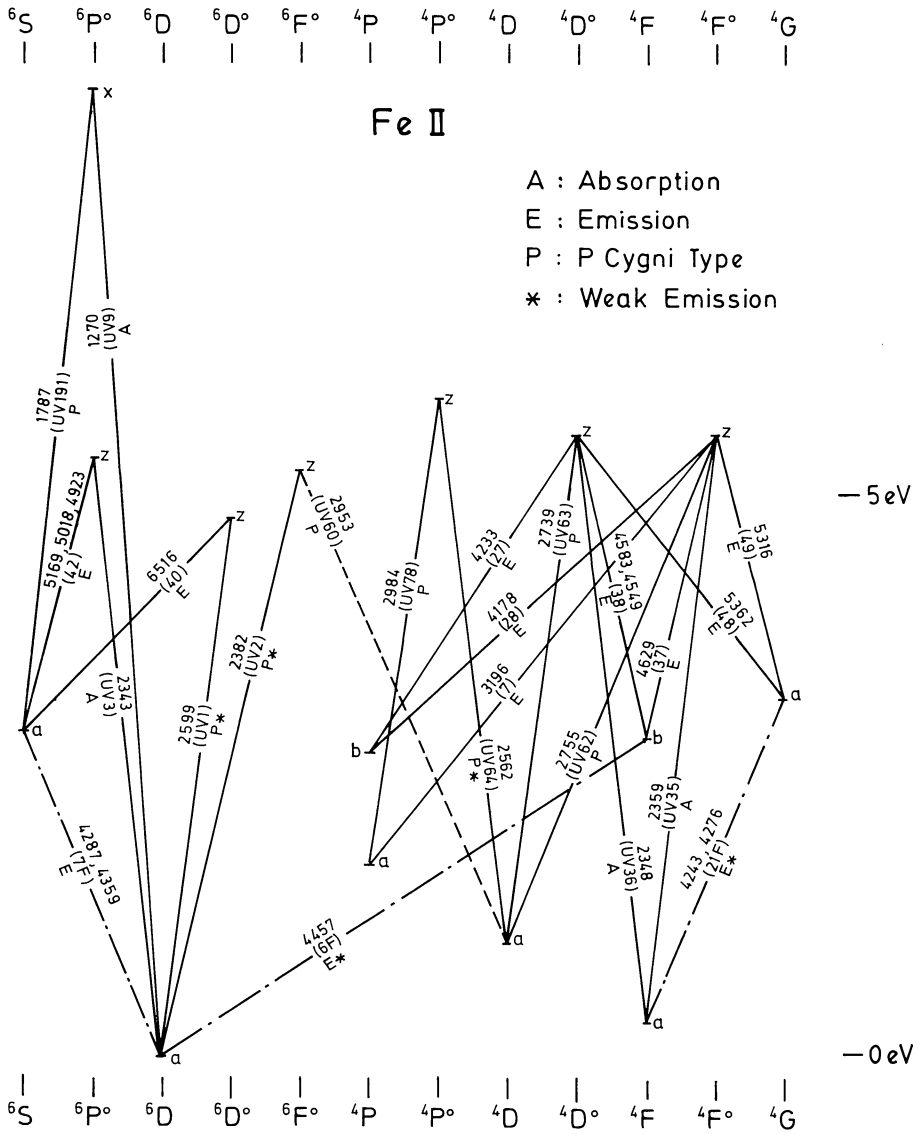

Fig. 14. Schematic partial Grotrian diagram of Fe II transitions, summarizing the different types of profiles observed in the spectrum of GG Car, and explaining the types of profile displayed in Figs. 12 and 13

phenomenon is straightforward when one looks at the partial Grotrian diagram displayed in Fig. 14.

The case of multiplet 191, $\lambda\lambda$ 1785-86-88 Å, which is conspicuous in the spectrum of GG Car, deserves a special mention. It is the only Fe II multiplet in the short wavelength spectrum that shows P Cyg type profiles while the remainder Fe II lines in this region are in absorption. The presence of the emission component can be interpreted as an excitation through radiative pumping via the Fe II resonance UV multiplet 9 at $\lambda\lambda$ 1260-76 Å ($a^6D - x^6P^0$) (Hempe and Reimers, 1982). Both multiplets, 9 and 191, have a common x^6P^0 upper level and since there are no further allowed downward transitions from x^6P^0, photons absorbed in the resonance multiplet decay to multiplet 191 in the high probability transition $x^6P^0 - a^6S$. As a direct consequence of the pumping mechanism, the intensity ratio of the emissions within the triplet indicates that the 1785.26 line could be expected to be nearly as strong as the 1786.74 line. But in the case of GG Car, the first line is stronger than the second one. The coincidence of Fe II 1260.54 (mult. 9) with the 1260.42 Si II line (mult. 4), which is also in absorption, may be responsible for that observed intensity ratio. This pumping effect can possibly account for the strength of the downward transitions between the $a^6S - a^6D$ levels into the forbidden [Fe II] $7F$ multiplet observed via its lines at $\lambda\lambda$ 4287.4, 4359.3 and 4413.8 Å (Swings, 1974; Hernandez et al., 1981; Gosset et al., 1985).

3.3.2. Mg II and O I emission lines

According to Bruhweiler et al. (1982, see their Fig. 3), a fluorescence mechanism (or Bowen mechanism) would also be responsible for the strong Mg II emissions observed in some Be stars (approximate coincidence of Ly β λ 1025.72 and of Mg II λ 1025.97 enabling an overpopulation of the Mg II $5p^2P^0$ level and downward cascade transitions producing the emission in the Mg II resonance lines).

The proof that the Bowen mechanism is efficient in the Mg II emission production is the presence of O I emission lines at λ 8446 Å and λ 1302 Å. In GG Car the first line is observed as a very strong emission in an ESO Reticon spectrum and the second one corresponds to multiplet 2 lines, which have P Cyg profiles according to the description given at the beginning of this paper. However, the subordinate Mg II lines observed in absorption are not in good agreement with the downward cascade scheme suggested by the Bowen mechanism. On the other hand, the presence of such a mechanism would mean that the Mg II emission lines arise in the same region as the hydrogen recombination spectrum.

3.4. Discussion of the high resolution spectrum

The absorption features observed in the UV spectrum of GG Car show a large range of values in widths of the line profiles, which probably originate from different regions. In the first place are almost undisplaced resonance lines of C I, S I, Cl I and Mn II which are very likely of interstellar origin and should be placed outside the proper domain of the system. Then come the components displayed by the lines arising from the 0.00 eV level of O I, Mg II, Fe II, etc. whose widths seem to be larger than those of C I or S I, although their velocities show a dispersion in the values depending on the given considered element (Table 2). These lines are probably formed in the outermost layers of the extended envelope; however the possibility exists that some of the lines have contributions of interstellar origin. At the other extreme, the UV spectrum of GG Car shows the broad lines of highly ionized species such as C IV and Si IV, with large expansion velocities (Table 2).

In the middle are the neutral elements like Mg I and O I, the singly ionized metals and the doubly ionized elements, whose widths increase as a function of their ionization. The observed UV line spectrum, therefore, corresponds to a large range in electron temperatures.

One characteristic of the UV spectrum of GG Car is the presence of a double structure in the Fe II and Ni II absorption features in the LWR images, which correspond to the phases 0.41 and 0.46 in the lightcurve, i.e. around the time of periastron when the "glitch" in the lightcurve as well as the double H absorption and He I absorption lines in the optical spectrum are observed (Gosset et al., 1985). The second component of the Balmer lines appears around phase 0.45 and may last up to phase 0.65 with a velocity of $-99\,\mathrm{km\,s^{-1}}$ (Gosset et al., 1985). The difference between the velocity of that component and the velocity of the center of gravity for the main component is about $40\,\mathrm{km\,s^{-1}}$. In the UV region, the same value is observed for the separation in the Fe II and Ni II absorptions. If we consider the possible relations between the behaviours of the Balmer lines and of the metallic ones, the observed effect should be related to the phases. In that case, the SWP image would show also splitting in the Fe II and Ni II lines. Moreover, it is not possible for these lines to arise in the same region, the Balmer lines being probably formed in deeper regions. It would be necessary to have a better coverage of the orbital cycle if we wished to relate the UV spectrum characteristics and variations observed in the visual region. Presently, the limited number of UV spectra does not enable us to derive a model of the extended atmosphere of this peculiar emission-line object.

4. The low resolution data: the UV continuum of GG Car

It is to be noted first that, for the low resolution data listed in Table 1b, all the spectra do appear very similar, once the few bad pixels have been removed; furthermore the spectra in the short- and in the long-wavelength regions reproduce well in their overlap zones, which gives a fair degree of confidence in the quality of the data calibration. The main absorption features that are visible between 1200 and 3300 Å are due to Ly α, to the resonance lines of C IV and Si IV, and to the important interstellar "bump" centered around 2200 Å.

The five pairs of data obtained through the large aperture and at the same phase in both wavelength regions, have been corrected for the 2200 Å "bump", assuming that the latter is of classical interstellar origin. The five corrections were performed independently, using the mean galactic extinction fit of Seaton (1979). The resulting excess E_{B-V} is 0.52 ± 0.04 (2σ), where the error comes from the measurement accuracy on the individual spectra; variations from one spectrum to the other never exceed this value. The $B - V$ excess obtained here is in good agreement with the value deduced by ourselves from the ANS satellite data (Thé et al., unpublished); in fact the overall shape of the UV continuum obtained with IUE is in excellent agreement with the ANS broad band photometric data.

As indicated above the IUE low resolution spectra appear to be very similar; it is the whole continuum that seems to vary with time. In order to be more specific about such variations, we defined two numerical rectangular filters avoiding the main absorptions, one being in the short wavelength region,

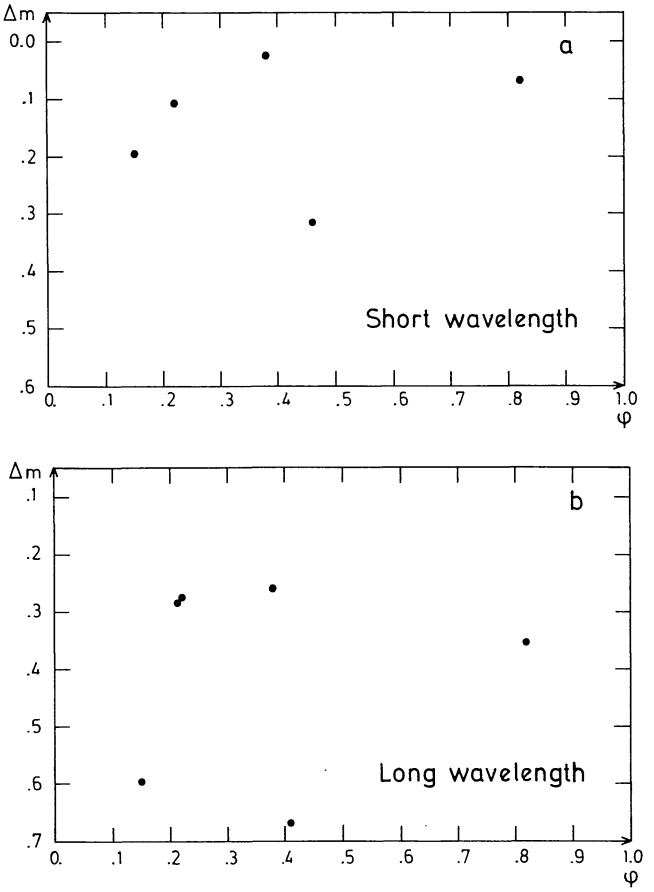

Fig. 15a and b. The ultraviolet lightcurve of GG Car; **a** centered around 1510 Å; **b** centered around 3230 Å available on the basis of IUE data

$\lambda \in [1493-1540\,\text{Å}]$, the other in the long wavelength zone, $\lambda \in [3200-3260\,\text{Å}]$: relative magnitudes (to the admitted IUE accuracy of 10–15%) were then computed for these two narrow regions. Although the number of data is fairly scarce, the result shown in Fig. 15 (a and b) clearly indicates that the UV continuous flux from GG Car does not vary with the epoch of the observation (see Table 1b) but rather with the phase along the lightcurve. In fact the UV lightcurve is very similar to that in the visible, with a broad primary minimum and a "glitch" around $\varphi = 0.45$. Unfortunately, the two spectra (SWP and LWR) obtained at the time of the "glitch" correspond to slightly different phases (0.46 and 0.41 respectively); it appears, however, that the "glitch" is definitely more pronounced in the ultraviolet than in the visible (see Fig. 3a of Gosset et al., 1985). Does this imply that we fortuitously "resolved" the "glitch"? No definite answer can be given, although this result strengthens a little the argument that the "glitch" is caused by a geometrical effect (Gosset et al., 1985). From Fig. 15 one may possibly infer that a slight change exists in the slope of the continuum, but the significance of this is difficult to establish.

An attempt was finally made to reproduce the continuous energy distribution of GG Car, from the ultraviolet to the visible (Johnson V filter) with model atmosphere predictions. Standard models of Kurucz (1979) were used: although not perfect, the best fit is obtained with a model for which $T_{\text{eff}} \simeq 18{,}000$ K. The gravity appears harder to determine, the preferred value being $\log g \simeq 4$. These approximate values are naturally to be taken with caution due to the large uncertainties in model atmospheres stressed by Kurucz (1986).

5. Concluding remarks

A summary of this paper is given in the fairly detailed abstract, to which we therefore refer the reader.

Clearly, however, the next step towards an understanding of a physical model of GG Car consists in an investigation of the ultraviolet radial velocity curve(s) of this intriguing object: to complete such a task, a very good coverage in phase is, of course, needed. A comparison to the variation of the H_α profile along the light curve will then be possible as well, since, for the latter, telescope time has recently been allocated. All these data will hopefully enable us to obtain a more quantitative physical model of the peculiar emission-line star GG Car.

Acknowledgements. We are indebted to W. Wamsteker and A. Cassatella for having very rapidly provided us with the archive IUE data, to the referees M. Hack and C. de Jager for their constructive remarks, and to M. Klutz for her preliminary work on the original IUE data.

One of the authors (EB) thanks the hospitality of the Institut d'Astrophysique at Liège where this work was carried out. Financial support from the Université de Liège and the IAU Exchange of Astronomers Program is gratefully acknowledged.

EG thanks the Fondation Mathieu of the Université de Liège and the Fondation Liégeois of the Académie Royale des Sciences de Belgique for financial support. Prof. M. Migeotte played a key role in making the latter grant available.

References

Allen, D.A.: 1973, *Monthly Notices Roy. Astron. Soc.* **161**, 145
Beals, C.S.: 1951, *Publ. Dominion Astrophys. Obs.* **9**, No. 1
Boggess, A. et al.: 1978a, *Nature* **275**, 372
Boggess, A. et al.: 1978b, *Nature* **275**, 377
Bohlin, R.C., Holm, A.V.: 1981, ESA IUE Newsletter **11**, 18
Bouchet, P., Swings, J.P.: 1982, in Be Stars, IAU Symp. **98**, eds. M. Jaschek, H.G. Groth, p. 241
Brandi, E., Gosset, E.: 1986, *Astron. Astrophys. Suppl. Ser.* (in press)
Bruhweiler, F.C., Morgan, T.H., van der Hucht, K.A.: 1982, *Astrophys. J.* **262**, 675
Cannon, A.J.: 1915, *Harvard Ann.* **76**, 31
Carlson, E.D.: 1968, Ph.D. Dissert., Northwestern Univ.
Carlson, E.D., Henize, K.G.: 1979, *Vistas in Astron.* **23**, 213
Cassatella, A., Ponz, D., Selvelli, P.L.: 1981, ESA IUE Newsletter **10**, 31
Chen, K.Y., Kowalske, K., Austin, R.R.D.: 1983, *Publ. Astron. Soc. Pacific* **95**, 157
Cohen, M., Barlow, M.J.: 1980, *Astrophys. J.* **238**, 585
de Freitas Pacheco, J.A., Faria Lopez, D., Landaberry, S.C., Selvelli, P.L.: 1985, *Astron. Astrophys.* **152**, 101
Gaposchkin, S.: 1953, *Harvard Ann.* **113**, No. 2
Gosset, E., Surdej, J., Swings, J.P.: 1984, *Astron. Astrophys. Suppl. Ser.* **55**, 411
Gosset, E., Hutsemékers, D., Surdej, J., Swings, J.P.: 1985, *Astron. Astrophys.* **153**, 71
Greenstein, N.K.: 1938, *Harvard Bull.* **908**, 25
Hack, M., Selvelli, P.L.: 1982, *Astron. Astrophys.* **107**, 200
Hempe, K., Reimers, D.: 1982, *Astron. Astrophys.* **107**, 36

Hernandez, C.A., Lopez, L., Sahade, J., Thackeray, A.D.: 1981, *Publ. Astron. Soc. Pacific* **93**, 747
Hoffleit, D.: 1933, *Harvard Bull.* **892**, 19
Holm, A.V.: 1982, NASA IUE Newsletter **18**, 10
Kruytbosch, W.E.: 1930, *Bull. Astron. Inst. Neth.* **6**, 11
Kurucz, R.: 1979, *Astrophys. J. Suppl. Ser.* **40**, 1
Kurucz, R.: 1986, in Highlights of Astronomy, Reidel Publ. Co., ed. J.-P. Swings, p. 827
Pickering, E.C.: 1896a, *Astron. Nachr.* **141**, 169
Pickering, E.C.: 1896b, Harvard Circ., No. 9 (also *Astrophys. J.* **4**, 142).
Sahade, J., Brandi, E.: 1985, *Rev. Mexicana Astron. Astrof.* **10**, 229
Sanduleak, N., Stephenson, C.B.: 1973, *Astrophys. J.* **185**, 899
Seaton, M.J.: 1979, *Monthly Notices Roy. Astron. Soc.* **187**, 73P
Selvelli, P.L., Stalio, R.: 1980, in 2nd European IUE Conference ESA/S.P. 157, p. 155
Smith, H.J.: 1955, Southern Wolf-Rayet Stars, Ph.D. Dissert., Harvard Univ.
Swings, J.P.: 1974, *Astron. Astrophys.* **34**, 333
Swings, J.P.: 1979, paper presented at ESA Fe II Workshop, Villafranca, Oct. 3–5, 1979, unpublished